Hybridization and correlation effects in the photoemission spectra of $R\mathrm{Ni}_2$ (R = Ce, Pr, and Nd)

J.-S. Kang, J. H. Hong, D. W. Hwang,* J. I. Jeong, S. D. Choi, C. J. Yang, and Y. P. Lee
Research Institute of Industrial Science and Technology, Pohang 790-600, Korea

C. G. Olson
Ames Laboratory, Iowa State University, Ames, Iowa 50011

Kicheon Kang and B. I. Min
Department of Physics, Pohang University of Science and Technology, Pohang 790-600, Korea
(Received 12 August 1993; revised manuscript received 1 December 1993)

Electronic structures of $R\mathrm{Ni}_2$ (R = Y, Ce, Pr, and Nd) are investigated systematically by using photoemission spectroscopy (PES) and compared with those of $R\mathrm{Co}_2$. Double-peak structures are observed in the R $4f$ PES spectra, in which the spectral weight near E_F decreases from Ce to Pr and Nd, suggesting a decrease in the R $4f$–Ni $3d$ hybridization from Ce to Pr and Nd. For the same R, the spectral weight near E_F in $R\mathrm{Ni}_2$ is smaller than that in $R\mathrm{Co}_2$, implying a smaller R $4f$ hybridization with Ni $3d$ electrons in $R\mathrm{Ni}_2$ than with Co $3d$ electrons in $R\mathrm{Co}_2$. These trends are consistent with those in the calculated hybridization matrix elements for RM_2 (M = Co and Ni). A pronounced Ni $3d$ satellite is observed, which arises from Ni $3d$ Coulomb correlation effects. The Ni $3d$ partial spectral weight distribution in $R\mathrm{Ni}_2$ exhibits important discrepancies from the calculated Ni $3d$ angular momentum projected local density of states (PLDOS), such as peak positions and line shapes, indicating substantial Ni $3d$ correlation effects. These discrepancies are qualitatively similar to, and quantitatively larger than, those for $R\mathrm{Co}_2$. Quasiparticle spectral densities are calculated by using the Hubbard Hamiltonian and including Co and Ni $3d$ electron correlation effects, which yield a better agreement with PES spectra than the local-density approximation PLDOS's.

I. INTRODUCTION

For rare earth (R) –transition metal (M) intermetallic compounds, it is generally considered that magnetic properties of R-cobalt (Co) or R-iron (Fe) compounds are primarily associated with Co or Fe sublattices, whereas in R-nickel (Ni) compounds, magnetic interactions involve only the R sublattice.[1,2] Magnetism of M $3d$ electrons in the R-M compounds can be described by itinerant magnetism, implying that M $3d$ electron Coulomb correlation effects are well described by one-electron band theory. Theoretical band structures of $\mathrm{Ce}M_2$ (M = Fe, Co, and Ni),[3] CeCo_5,[4] GdCo_5,[5] and $\mathrm{Nd}_2\mathrm{Fe}_{14}\mathrm{B}$,[6] obtained by using the local-density-functional approximation (LDA), support itinerant magnetism of M $3d$ electrons in these compounds. The calculated band structure of $\mathrm{Nd}_2\mathrm{Fe}_{14}\mathrm{B}$ also yields reasonably good agreement with Fe $3d$ spectra which are obtained by using photoemission spectroscopy (PES). In contrast, recent PES studies of $R\mathrm{Co}_2$ with R = Ce, Pr, and Nd,[7] indicate that there are substantial correlation effects not only among R $4f$ but also among Co $3d$ electrons, and that the estimated Co $3d$ Coulomb correlation energy (U_{dd}) is comparable to the Co $3d$ bandwidth. Thus it is still controversial whether magnetic properties and electronic structures of M $3d$ electrons in these compounds can be consistently described by a band theory. In addition, the role of R $4f$ electrons in magnetism in these compounds is not fully understood yet.

To resolve these issues, we extend our previous PES investigation of $R\mathrm{Co}_2$ to $R\mathrm{Ni}_2$ compounds (R = Ce, Pr, and Nd), which are structural counterparts of $R\mathrm{Co}_2$ but are magnetically simpler than $R\mathrm{Co}_2$ because Ni sublattices are nearly nonmagnetic. Studies of magnetic properties for $R\mathrm{Ni}_2$ indicate that YNi_2, CeNi_2, and PrNi_2 are paramagnetic, and NdNi_2 is ferromagnetic with a Curie temperature (T_C) $\sim$ 16 K.[1] Note for comparison that YCo_2 and CeCo_2 are paramagnetic, while PrCo_2 and NdCo_2 are ferromagnetic, with $T_C \sim$ 50 K and $\sim$ 120 K, respectively. Based on the systematic comparison of electronic structures of $R\mathrm{Ni}_2$ and $R\mathrm{Co}_2$, we have tried to correlate Co and Ni $3d$ Coulomb correlation effects with their electronic structures and magnetism. It is expected that correlation effects in the Ni $3d$ PES spectra will be more clearly identified because Coulomb correlation interactions among Ni $3d$ electrons in $R\mathrm{Ni}_2$ are known to be larger than those among Co $3d$ electrons in $R\mathrm{Co}_2$. Furthermore, the relation between R $4f$ spectral features and their magnetic properties may be separated out more easily in $R\mathrm{Ni}_2$ than in $R\mathrm{Co}_2$.

In this paper we report valence-band PES results for $R\mathrm{Ni}_2$, with R = Y, Ce, Pr, and Nd. This paper is organized as follows. In Sec. II, experimental and computational details are described. In Sec. III, PES results for $R\mathrm{Ni}_2$ are presented. In Sec. IV, hybridization interactions between R $4f$ and Co and Ni $3d$ electrons are discussed. The measured PES spectra of $R\mathrm{Ni}_2$ and $R\mathrm{Co}_2$

are compared with the angular-momentum-projected local densities of states (PLDOS's) which are obtained from band structure calculations. In order to examine the Co and Ni $3d$ electron Coulomb correlation effects on the LDA PLDOS, we present the quasiparticle spectral densities which are calculated by taking into account self-energy corrections in the context of the Hubbard model. Finally conclusions are summarized in Sec. V.

II. EXPERIMENTAL AND COMPUTATIONAL DETAILS

Polycrystalline samples of $R\mathrm{Ni}_2$ (R = Y, Ce, Pr, and Nd) were prepared by induction melting under argon gas atmosphere. To compensate the loss of R elements during melting, additional 10% of constituent R elements were weighed above the stoichiometric amounts. Samples were then encapsulated in vacuum-sealed quartz tubes, and were homogenized at 1000 °C for more than 24 h under vacuum. X-ray diffraction indicated that the samples were crystallized in the MgCu_2-type Laves phase,[8] with an impurity phase less than 5%. The details for synchrotron radiation photoemission measurements are same as those in Ref. 7. The samples were cleaved *in situ* and measured at $\sim$ 60 K in a vacuum better than 4×10^{-11} Torr. The overall instrumental resolution is about 0.3 eV at $h\nu \sim 50$ eV and 0.4 eV at $h\nu \sim 150$ eV, respectively.

Calculated $3d$ angular-momentum-projected local densities of states (PLDOS's) are obtained by using the self-consistent linearized muffin-tin-orbital (LMTO) band method within the LDA. We have assumed the paramagnetic phase for $R\mathrm{Ni}_2$, and utilized the Gaussian broadening method to get the density of states.

In obtaining the quasiparticle spectral density, we have used the Hubbard model in the weak correlation limit, i.e., $U/t < 1$ (U is the on-site Coulomb energy and t the bandwidth). The self-energy is calculated by employing the equation of motion method for the Green's function and the conventional decoupling procedure for the higher-order Green's function. Then the local approximation is utilized to evaluate the self-energy up to second order in U/t.[9] The quasiparticle spectral density is obtained by taking the imaginary part of the single-particle Green's function.[10] The details are described in Ref. 11.

III. RESULTS

Figures 1(a)–1(d) display valence-band energy distribution curves (EDC's) of $R\mathrm{Ni}_2$ with R = Y, Ce, Pr, and Nd, respectively, around the Ni $3p$ absorption edge. Between ~ -4 eV and the Fermi level E_F, Ni $3d$ emissions are dominant with a small contribution from R $4f$ emissions.[12] Note that the valence-band spectra of $R\mathrm{Ni}_2$ are similar one another, suggesting that the overall electronic structure due to non-$4f$ electrons is very similar in $R\mathrm{Ni}_2$. Broad features which appear at fixed kinetic energies, i.e., which shift away from E_F through the valence band as $h\nu$ increases, are due to Ni MVV Auger emis-

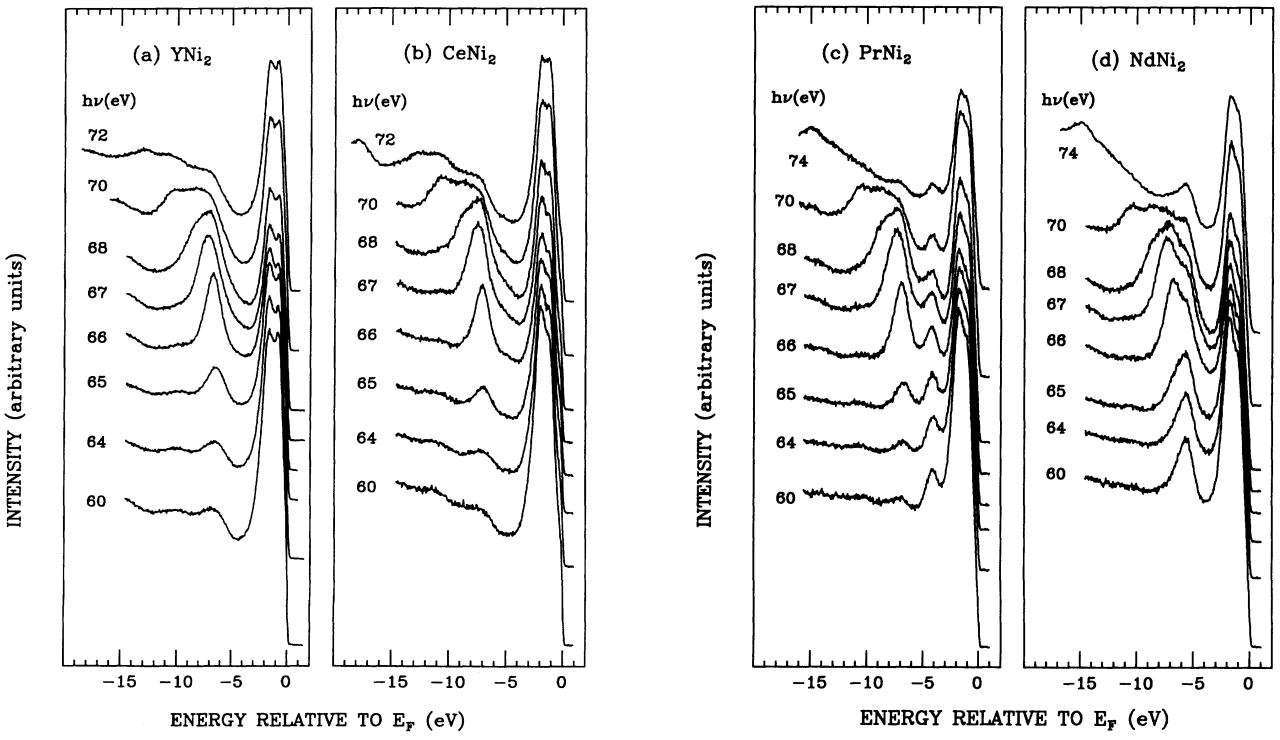

FIG. 1. Energy distribution curves (EDC's) for $h\nu$ near the Ni $3p \rightarrow 3d$ absorption edge (a) for YNi_2, (b) for CeNi_2, (c) for PrNi_2, and (d) for NdNi_2

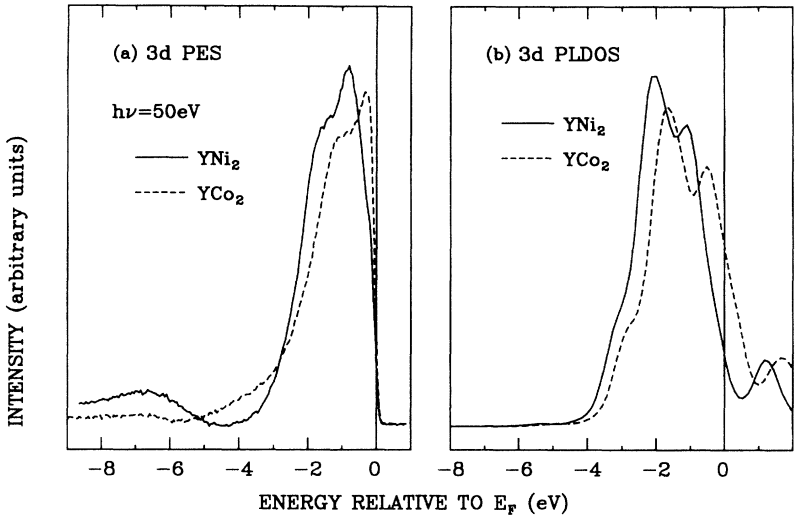

FIG. 2. (a) Comparison of the EDC's, taken at $h\nu = 50$ eV, for YNi_2 (solid lines) and YCo_2 (dashed lines). (b) Comparison of the calculated M $3d$ angular-momentum-projected densities of states (PLDOS's) for YNi_2 (solid lines) and for YCo_2 (dashed lines).

sions. For $h\nu = 72$ eV or 74 eV, where Ni MVV emissions are well below the valence band, a common feature near -7 eV is clearly observed (about 6 eV below the main Ni $3d$ valence band) except for $NdNi_2$. This emission is identified as the well-known Ni $3d$ satellite,[13–15] which arises from Ni $3d$ Coulomb correlation effects. The 6 eV satellite feature is obscured in $NdNi_2$ by overlapping Nd $4f$ emissions. The feature near -4 eV in $PrNi_2$ is due to Pr $4f$ emissions.

In order to compare essential features of Ni and Co $3d$ electronic structures of RM_2 (M = Ni and Co) compounds, we compare the $h\nu = 50$ eV spectra of YNi_2 and YCo_2 in Fig. 2(a), which are dominated by Ni and Co $3d$ emissions, respectively.[12] YNi_2 and YCo_2 are chosen because they do not have overlapping R $4f$ emissions. The spectra in this figure are scaled to each other so that the area underneath each curve is proportional to the number of M $3d$ electrons obtained in band structure calculations (8.57 for YNi_2 and 7.56 for YCo_2). Several differences are found in Fig. 2(a). First, the spectral weight of Ni $3d$ electrons at E_F is smaller than that of Co $3d$ electrons at E_F, and Ni $3d$ peak positions are shifted away from E_F compared to Co $3d$ peak positions (by ~ 0.5 eV). These differences reflect an increased filling of Ni $3d$ bands, as compared to Co $3d$ bands. Second, the Ni $3d$ spectrum exhibits a satellite emission at ~ -7 eV, whereas the Co $3d$ spectrum exhibits no weight near -7 eV but some weight around -4.5 eV, which was previously ascribed to a Co $3d$ satellite.[7] Therefore the energy separation between the $3d$ main band and the satellite in YNi_2 is larger than that in YCo_2. Third, the Ni $3d$ satellite structure in YNi_2 is more pronounced than the Co $3d$ satellite structure in YCo_2. The second and third features are due to a larger U_{dd} for Ni $3d$ electrons in RNi_2, as compared to Co $3d$ electrons in RCo_2, which is consistent with an expectation based on the study of pure Co and Ni metals.[16]

In Fig. 2(b), we compare calculated M $3d$ PLDOS's of YNi_2 and YCo_2, which are obtained from LDA band structure calculations, as described in Sec. II. As in Fig. 2(a), calculated $3d$ PLDOS's exhibit similar differences, which originate mainly from a different band filling between Ni and Co $3d$ bands, i.e., a smaller magnitude of the Ni $3d$ PLDOS at E_F with peak positions at higher binding energies, as compared to the Co $3d$ PLDOS. However, the satellite structures in the PES spectra are not explained by the calculated $3d$ PLDOS's, which will be further discussed in Sec. IV B in more detail.

Figure 3 displays the extracted R $4f$ PES spectra for RNi_2 (solid lines), in comparison with those for RCo_2

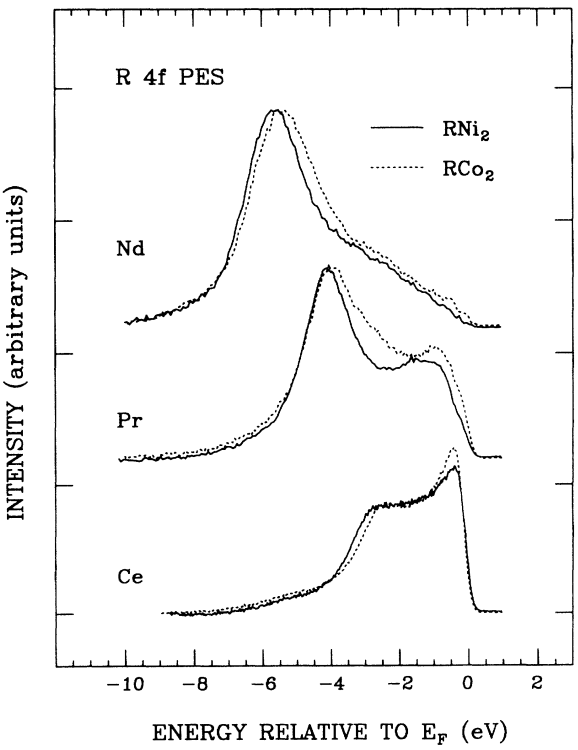

FIG. 3. Extracted R $4f$ PES spectra of RNi_2 (solid lines), in comparison to those of RCo_2 (dashed lines), which are taken from Ref. 7, with R = Ce, Pr, and Nd.

(dashed lines), with R = Ce, Pr, and Nd. The extraction procedures are explained in Ref. 7. Results for $R\mathrm{Ni}_2$ are new, and those for $R\mathrm{Co}_2$ are taken from Ref. 7. Several interesting features are observed. (i) The extracted $4f$ PES spectra exhibit double-peak structures, i.e., one well below E_F and the other near E_F, in which the spectral weight near E_F decreases from Ce to Pr and Nd for both $R\mathrm{Ni}_2$ and $R\mathrm{Co}_2$. The peaks well below E_F correspond to the trivalent R $4f^n \rightarrow 4f^{n-1}$ transitions.[17] Note that pure Pr metal exhibits two peaks attributable to $4f$ electrons,[18] similar to the structures observed in Ce materials. The peaks near E_F are known to arise from hybridization effects between R $4f$ and conduction electrons.[19–22] (ii) For the same R, the spectral intensity near E_F relative to that of the trivalent peak is lower in $R\mathrm{Ni}_2$ than in $R\mathrm{Co}_2$. Further, the FWHM (full width at half maximum) of the trivalent peak in $R\mathrm{Ni}_2$ is narrower than that in $R\mathrm{Co}_2$ (R = Pr and Nd). The linewidths of trivalent R $4f$ peaks and the features near E_F will be further discussed in Sec. IV A. (iii) The positions of the trivalent R $4f^n \rightarrow 4f^{n-1}$ transitions (ϵ_f) in these compounds are shifted to slightly higher binding energies (by ~ 0.5 eV), as compared to pure rare earth metals.[23]

IV. DISCUSSION

A. Hybridization effects in R $4f$ spectra

In the previous section, it was mentioned that the FWHM's of trivalent R $4f$ PES peaks in $R\mathrm{Ni}_2$ are narrower than those of $R\mathrm{Co}_2$ (R = Pr and Nd). Differences in the trivalent R $4f$ linewidths of $R\mathrm{Ni}_2$ and $R\mathrm{Co}_2$ may arise from the differences in the following factors: (i) hybridization between R $4f$ and near neighbor M $3d$ electrons, (ii) a lifetime broadening due to an Auger recombination,[24] (iii) the presence of surface-shifted trivalent R $4f$ emissions,[23,25,26] or (iv) an inhomogeneity of the samples due to the presence of grain boundaries, which is estimated to be less than 5%.

Hybridization broadening of the R $4f$ spectrum depends on the magnitude of the hybridization matrix element and the valence-band DOS at the energy position of the R $4f$ transitions.[19] As will be discussed below in Table I, the calculated hybridization matrix elements for $R\mathrm{Co}_2$ are larger than those for $R\mathrm{Ni}_2$, supporting hybridization broadening as one of the possible mechanisms for the trivalent R $4f$ peak widths. Regarding the second possibility, there is a large probability of an interatomic Auger process for RM_2 (M = Co and Ni), as compared to pure R metals. This is because the total number of valence-band electrons in RM_2 is larger than that in pure R metals, mainly due to Co and Ni $3d$ electrons, which will lead to interatomic Auger recombination.[24] However, the number of Ni $3d$ electrons is larger than that of Co $3d$ electrons, making lifetime effects a less likely cause for differences between $R\mathrm{Ni}_2$ and $R\mathrm{Co}_2$. As for the surface contribution to the linewidth, the PES spectra of RM_2 (M = Ni and Co) are expected to be more surface sensitive than those for pure R metals, since the electron mean free paths in RM_2 are considerably smaller than those in pure R metals due to increased electron densities.[27] Thus it is essential to include the surface effects in the quantitative analysis of the valence-band PES spectra.[28] Recently, Laubschat *et al.*[25,26] provided direct evidence of these surface effects, and showed that, for α-like Ce materials, surface electronic structures are almost γ-like. Therefore, it is possible that *surface* contributions might be dominant in the trivalent PES peaks for CeCo_2 and CeNi_2. For heavier rare earths, it is more likely that both *bulk* and *surface* components contribute to the trivalent R $4f$ PES peaks.[6,23,29] In addition, the *surface* to *bulk* emission ratios are expected to be similar for $R\mathrm{Co}_2$ and $R\mathrm{Ni}_2$.

TABLE I. Crystal structure data of the R-M distances $d_{R\text{-}M}$ (Å), calculated MTO radii of M $3d$, r_d (Å), and R $4f$, r_f (Å), and calculated matrix elements V_{df} (eV).

		$d_{R\text{-}M}$	r_d	r_f	V_{df}
$R\mathrm{Co}_2$	CeCo_2	2.969	0.557	0.572	0.161
	PrCo_2	3.031	0.557	0.546	0.127
	NdCo_2	3.026	0.556	0.526	0.117
	SmCo_2	3.010	0.556	0.492	0.102
	GdCo_2	3.009	0.555	0.464	0.088
$R\mathrm{Ni}_2$	CeNi_2	2.995	0.532	0.572	0.143
	PrNi_2	3.020	0.532	0.547	0.121
	NdNi_2	3.013	0.531	0.528	0.113
	SmNi_2	2.999	0.531	0.494	0.098
	GdNi_2	2.988	0.530	0.465	0.086

In the Ce $4f$ PES spectra of CeCo_2 and CeNi_2, large spectral weights near E_F are typical of other cerium materials which have large hybridization. In the band theoretical view, the peaks near E_F are interpreted as the ground-state R $4f$ bands, corresponding to fully relaxed $4f$ spectra.[21] On the other hand, this may be understood in terms of the degenerate impurity Anderson Hamiltonian, developed by Gunnarsson and Schönhammer (GS),[19] which has provided a coherent description of both spectroscopic and certain ground-state properties of Ce and Yb materials.[19,20,28,30,31] In this model, the spectral features close to E_F originate from the hybridization between R $4f$ and conduction-band electrons and also from on-site Coulomb interaction energy among R $4f$ electrons (U_{ff}). For CeNi_2 and CeCo_2 in particular,[32] the peaks near E_F are associated with Kondo resonances of nonmagnetic singlet ground states. For $\mathrm{Pr}M_2$ and $\mathrm{Nd}M_2$, however, the structures near E_F are not associated with Kondo-like effects.

Note that relative intensities near E_F in $R\mathrm{Ni}_2$ are lower than those in $R\mathrm{Co}_2$. We speculate that such differences reflect a smaller R $4f$–Ni $3d$ hybridization in $R\mathrm{Ni}_2$ than R $4f$–Co $3d$ hybridization in $R\mathrm{Co}_2$. This speculation is based on the assumptions that the trivalent R $4f$ PES peaks are composed of *bulk* and *surface* components, and that the ratio of *surface* to *bulk* contributions is similar in $R\mathrm{Ni}_2$ and $R\mathrm{Co}_2$ for the same R. Such an interpretation is consistent with the calculated hybridization matrix elements in Table I. This is probably because Ni $3d$ electron wave functions are more localized than Co $3d$ electron wave functions, and so the overlap of R $4f$ and Ni $3d$ wave functions is smaller than that of R $4f$ and

Co 3*d* wave functions (see Table I and Fig. 4), yielding smaller *R* 4*f*–Ni 3*d* hybridization. Under the same assumptions, it can be understood that the observed shift of $|\epsilon_f|$ in RM_2 (R = Pr and Nd), as compared to pure rare earth metals, is due to the large *R* 4*f*–*M* 3*d* hybridization which might push *R* 4*f* states away from *M* 3*d* states.[33] Another possible reason for the observed shift of $|\epsilon_f|$ is a larger *surface* emission contribution in RM_2, in which *surface R* 4*f* levels are shifted to higher binding energies with respect to *bulk R* 4*f* levels.

The magnitude of the *R* 4*f*–*M* 3*d* hybridization can be estimated by assuming that the *R* 4*f*–*M* 3*d* hybridization depends on (i) the energy difference of *R* 4*f* and *M* 3*d* states, (ii) the distance between *R* 4*f* and *M* 3*d* atoms in the crystal structure, and (iii) the number of nearest neighbors. For RM_2 compounds, the number of nearest neighbors does not change as R or M varies, and so the former two factors contribute. The relative importance of the two factors can be quantified by following an approach by Harrison and Straub.[34,35] This formalism combines Andersen's muffin-tin-orbital theory[36] with transition metal pseudopotentials[37] to obtain a general hybridization matrix element $V_{l,l',m}$,

$$V_{l,l',m} = (\eta_{l,l',m}\hbar^2/m_e)[(r_l^{2l-1}r_{l'}^{2l'-1})^{1/2}/d^{l+l'+1}], \quad (1)$$

where m is the angular momentum about the axis between the two atoms (in units of $\hbar$), m_e is the electron mass, and $\eta_{l,l',m}$ is the coupling coefficient which depends on the bond characteristic. The form of $\eta_{l,l',m}$ is given by Eq. (B2) in Ref. 35. Input parameters in Eq. (1) are angular momenta l and l' (l = 2 for d and l = 3 for f orbitals), the effective radii of the respective orbitals r_l and $r_{l'}$, and the interatomic distance d. In calculating hybridization matrix elements for RM_2 (R = light rare earth; M = Co and Ni) using the above formalism, we have used the crystal structure data for the interatomic distance between R and M atoms.

For r_l and $r_{l'}$, we have used expectation values of the radial distances for the radial wave functions R_l and $R_{l'}$, respectively, obtained from the LDA ground-state charge density by treating all electrons as core electrons. These values characterize the average distance from the nuclei for each orbital. As an example, the calculated radial probability density functions $[P_l(r) = 4\pi|rR_l(r)|^2]$ are provided in Fig. 4 for $CeCo_2$ and $CeNi_2$, as a function of distance from the nucleus. One can see that Ce $P_{4f}(r)$ exhibits a steeper decrease and a much smaller spread, as compared to Ce $P_{5d}(r)$. Note that *M* $P_{3d}(r)$ overlaps substantially with Ce $P_{5d}(r)$, but little with Ce $P_{4f}(r)$, suggesting that there would be a large hybridization interaction between Co or Ni 3*d* and Ce 5*d* states,[3] and that Co or Ni 3*d* states interact with Ce 4*f* states via Ce 5*d* states.

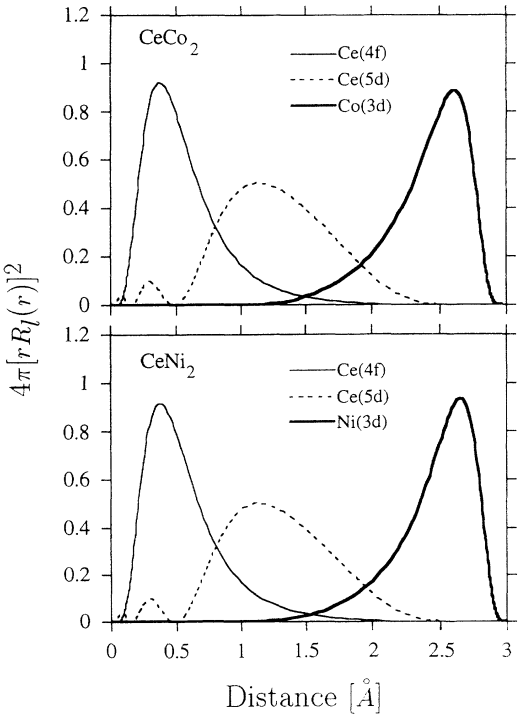

FIG. 4. Top: Radial probability density functions of $4\pi|rR_l|^2$ for Ce 4*f*, Ce 5*d*, and Co 3*d* states, where R_l denotes a corresponding radial wave function for $CeCo_2$. Ce and Co atoms are separated by an amount corresponding to the interatomic distance. Bottom: Similarly for $CeNi_2$.

Table I summarizes the calculated hybridization matrix elements V_{df} between *R* 4*f* and *M* 3*d* states for m = 0. We have dropped the index m, because it is sufficient to calculate only the σ bonds (m = 0) in order to describe trends. This table reveals that *R* 4*f*–*M* 3*d* hybridization decreases as R becomes heavier, and is smaller in RNi_2 than in RCo_2. These trends are consistent with those found in *R* 4*f* spectra of RM_2 (see Fig. 3), i.e., the *R* 4*f* spectral weight near E_F decreases as R varies from Ce to Pr and Nd, and as M varies from Co to Ni. A smaller value of the calculated hybridization between Ce 4*f* and Ni 3*d* states, as compared to that of Ce 4*f* and Co 3*d* states, is also consistent with the finding in Fig. 4 that the Ni 3*d* wave function is more localized than the Co 3*d* wave function.

B. Effects of Co and Ni 3*d* Coulomb correlation interactions

In order to find whether a band theory consistently describes both magnetic properties and electronic structures of Co and Ni 3*d* states, we now compare the calculated density of states with measured PES spectra. Figure 5 compares the PES spectra of RM_2 with the calculated *M* 3*d* PLDOS's (R = Y, Ce, Pr, and Nd; M = Ni and Co). Dots denote the PES spectra, taken at Fano minima of *R* 4*f* cross sections,[38] which represent *M* 3*d* emissions. An inelastic background has been subtracted from each PES spectrum. Solid lines denote the calculated 3*d* PLDOS's for paramagnetic phases.

It is found that the FWHM of the calculated PLDOS is comparable to that of the PES spectrum (about 2 eV) in each compound, even though more correct conclusions should be drawn by including both occupied and unoccupied parts, which requires combination of PES and IPES

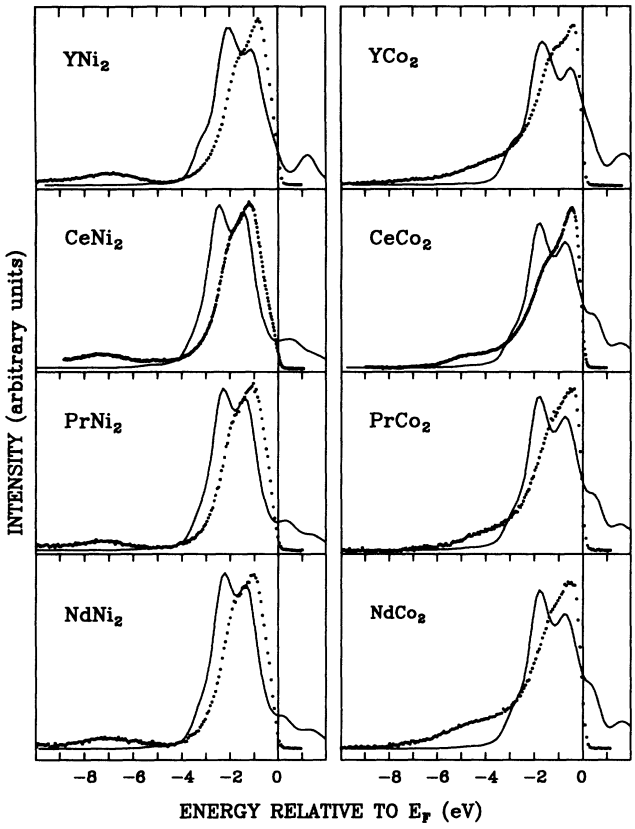

FIG. 5. Comparison of Ni $3d$ PES spectra (dots), taken at Fano minima of R $4f$ cross sections, with the calculated Ni $3d$ PLDOS's (solid lines) for $R\mathrm{Ni}_2$ (R = Y, Ce, Pr, and Nd). A similar comparison is shown for $R\mathrm{Co}_2$ (taken from Ref. 7) in the right panel.

(inverse photoemission spectroscopy), or bremsstrahlung isochromat spectroscopy (BIS) spectra. A comparable magnitude of FWHM implies a rather delocalized nature of Ni and Co $3d$ electrons. On the other hand, several disagreements are found between band theoretical results and measured PES spectra, suggesting the importance of $3d$ electron Coulomb correlation effects in these compounds. First, calculated peak positions are located at higher binding energies than experimental ones. Second, line shapes of occupied parts of $3d$ PLDOS's are substantially different from those of $3d$ PES spectra. Part of such discrepancies may be due to matrix element effects,[39,40] which are not included in the theory curves. Third, extra spectral weights in high binding energy regions of $3d$ PES spectra are not explained by the calculated PLDOS's. Extra spectral weights in PES spectra are located at ~ -7 eV and at ~ -4.5 eV in $R\mathrm{Ni}_2$ and $R\mathrm{Co}_2$, respectively. Note that these positions correspond to the locations of Ni and Co $3d$ satellite emissions.

We speculate that observed discrepancies between calculated $3d$ PLDOS's and $3d$ PES spectra originate mainly from Coulomb correlation effects among Ni and Co $3d$ electrons in both $R\mathrm{Ni}_2$ and $R\mathrm{Co}_2$. Indeed, the observed discrepancies in peak positions and spectral weight distributions are larger in $R\mathrm{Ni}_2$ than in $R\mathrm{Co}_2$, which supports our speculation that Coulomb correlation energy among Ni $3d$ electrons is larger than that among Co $3d$ electrons. An analogous behavior was observed in angle-resolved photoemission studies of pure transition metals,[41] i.e., that $3d$ electron Coulomb correlation effects increase from Fe to Co and Ni. Energy separations between the main bands and the satellites in the $3d$ PES spectra of $R\mathrm{Ni}_2$ and $R\mathrm{Co}_2$ are comparable to those of Ni and Co metals, respectively.[42] Therefore U_{dd} values for $R\mathrm{Co}_2$ and $R\mathrm{Ni}_2$ are expected to be comparable to those for Co and Ni metals,[16,42,43] which is confirmed by our analysis below.

In order to study the influence of Co and Ni $3d$ electron Coulomb correlations on band structure calculations, we have calculated quasiparticle spectral densities for YM_2 (M = Co and Ni) within the framework of the Hubbard model, as described in Sec. II. We have calculated self-energies as a function of U/t, and obtained the spectral densities using the Co and Ni $3d$ PLDOS's for YCo_2 and YNi_2 as input noninteracting densities. The results show a trend that, as U/t increases, the bandwidth becomes narrower and new structures (satellite peaks) appear, consistent with our expectation.

Figure 6 shows the calculated quasiparticle spectral densities for YCo_2 and YNi_2 for those U values which agree best with experiments. For YCo_2 (top panel), the

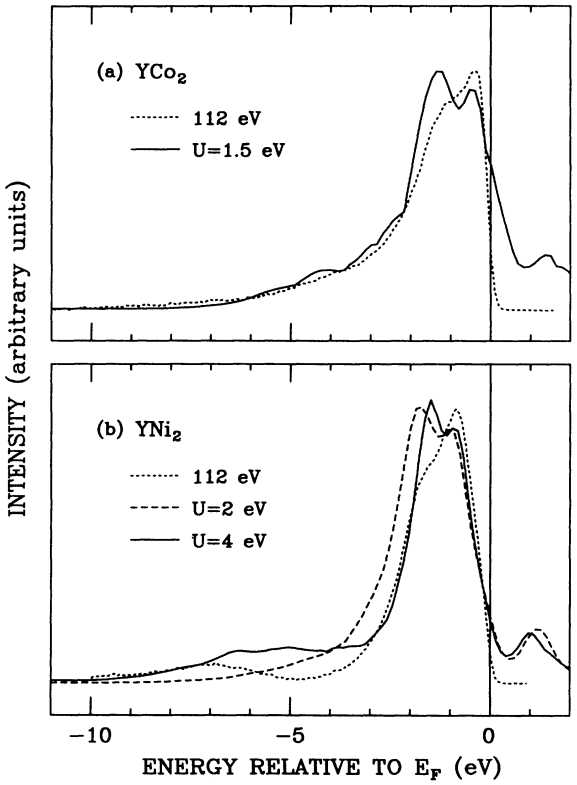

FIG. 6. (a) Comparison of the quasiparticle spectral density (solid lines) with the PES spectrum (dots) for YCo_2. The quasiparticle spectral density is calculated for U = 1.5 eV, by using the LDA Co $3d$ PLDOS for YCo_2. (b) Similarly for YNi_2. Solid and dashed lines denote the quasiparticle spectral densities for U = 4 eV and 2 eV, respectively, obtained by using the Ni $3d$ PLDOS for YNi_2.

quasiparticle spectrum with $U = 1.5$ eV agrees well with the PES spectrum. Good agreements are found not only for the Co 3*d* bandwidth but also for the peak positions and the spectral weight near -4.5 eV, which were the main discrepancies between the Co 3*d* PLDOS and PES spectrum (see Fig. 5). In contrast, for YNi_2 (bottom panel), the quasiparticle spectra with U between 2 eV and 4 eV do not show such a good agreement with the Ni PES spectrum. For $U = 2$ eV, no satellite structure has appeared yet in the quasiparticle spectrum, suggesting that $U = 2$ eV is still too small for YNi_2. For $U = 4$ eV, there are conflicting features. First, the total bandwidth of the quasiparticle spectrum becomes too narrow (unoccupied part of the band is not seen in the PES spectrum) and the separation between the two peaks in the main band becomes smaller than that in the PES spectrum, suggesting that the U value should be smaller. On the contrary, the separation between the satellite and the main band in the quasiparticle spectrum is smaller than that in the PES spectrum, indicating that a larger value of U is required.

Calculated quasiparticle spectral densities reveal how Co and Ni 3*d* electron correlation effects influence their LDA PLDOS's. The above analysis yields the on-site 3*d* Coulomb correlation energy for YCo_2 to be $\sim$ 1.5 eV and that for YNi_2 to be $\sim$ 2 eV to $\sim$ 4 eV. These values are close to the estimated values for pure Co and Ni metals.[16,42,43] Note that U_{dd} for RCo_2 and RNi_2 turns out to be comparable to Co and Ni 3*d* bandwidths in the order of magnitudes. A possible origin for the difficulty in obtaining a good agreement between the quasiparticle spectral density and the PES spectrum for YNi_2 seems to be that our treatment of the Hubbard model in the weak correlation limit may not work for YNi_2, for which U_{dd} is comparable to or even larger than the bandwidth.

V. CONCLUSIONS

Large-energy-scale features in Ni 3*d* PES spectra are found to be essentially identical for RNi_2 with R = Y, Ce, Pr, and Nd, which indicates that their 3*d* electronic structures are similar. Strong Ni *MVV* Auger emissions are observed, with intensity enhancement near the Ni 3*p* absorption edge, and a pronounced Ni 3*d* satellite is observed for RNi_2. Both features reflect Ni 3*d* Coulomb correlation effects. The calculated Ni 3*d* PLDOS's are compared with the Ni 3*d* PES spectra for RNi_2, in which the Ni 3*d* bandwidths exhibit reasonably good agreement between theory and experiment. On the other hand, the calculated 3*d* PLDOS's for RNi_2 also exhibit certain discrepancies from experiments, in peak positions and in weight distributions, similar to the case of RCo_2. These discrepancies are larger for RNi_2 than for RCo_2, implying a larger Ni 3*d* Coulomb correlation than for Co 3*d*. Thus this comparison suggests that Co and Ni 3*d* correlation effects are important in determining their electronic structures. Indeed, such conjecture is supported by an analysis in which quasiparticle spectral densities are calculated for YCo_2 and YNi_2 as a function of on-site Coulomb interaction energy (U_{dd}) within the framework of the Hubbard Hamiltonian. Calculated quasiparticle spectral densities provide evidence of large correlation effects of Co and Ni 3*d* electrons, in showing better agreement with the PES spectra than LDA PLDOS's do. In this analysis, 3*d* electron Coulomb correlation energies are estimated to be $\sim$ 1.5 eV for YCo_2, and $\sim$ 2 eV to $\sim$ 4 eV for YNi_2.

Double-peak structures are observed in the R 4*f* PES spectra of RNi_2 (R = Ce, Pr, and Nd), in which the spectral weight near E_F decreases from Ce to Pr to Nd. For the same R, the spectral weight near E_F in RNi_2 is smaller than that in RCo_2. The former trend implies that the localization of the R 4*f* wave function increases from $CeNi_2$ to $PrNi_2$ and $NdNi_2$. The latter trend indicates that the R 4*f* hybridization with Ni 3*d* electrons in RNi_2 is smaller than that with Co 3*d* electrons in RCo_2, suggesting a larger contribution of the localized R 4*f* moment in RNi_2 than in RCo_2. These trends are found to be consistent with the calculated values of hybridization matrix elements for RM_2 (R = light rare earths; M = Co and Ni).

ACKNOWLEDGMENTS

We thank J.-G. Park for helpful discussions. The photoemission experiment was carried out at the Synchrotron Radiation Center (SRC) of the University of Wisconsin–Madison. Travel funds to SRC were provided by the Pohang Light Source (PLS). This work was supported by the Korean Science and Engineering Foundation under Contract No. 921-0200-005-2 and also by the POSTECH-BSRI program of the Korean Ministry of Education.

* Permanent address: Department of Physics, Gyeongsang National University, Chinju 660-701, Korea.

[1] W.E. Wallace, *Rare Earth Intermetallics* (Academic Press, New York, 1973).
[2] *Ferromagnetic Materials*, edited by E.P. Wohlfarth and K.H.J. Buschow (North-Holland, Amsterdam, 1988).
[3] O. Eriksson, L. Nordstroem, M.S.S. Brooks, and B. Johansson, Phys. Rev. Lett. **60**, 2523 (1988).
[4] L. Nordstroem, O. Eriksson, M.S.S. Brooks, and B. Johansson, Phys. Rev. B **41**, 9111 (1990).
[5] B.I. Min (unpublished).
[6] B.I. Min, J.-S. Kang, J.H. Hong, S.W. Jung, J.I. Jeong, Y.P. Lee, S.D. Choi, W.Y. Lee, C.J. Yang, and C.G. Olson, Phys. Rev. B **48**, 6217 (1993).
[7] J.-S. Kang, J.H. Hong, J.I. Jeong, S.D. Choi, C.J. Yang, Y.P. Lee, C.G. Olson, B.I. Min, and J.W. Allen, Phys. Rev. B **46**, 15 689 (1992).
[8] *Crystallographic Data on Metal and Alloy Structures*, edited by A. Taylor and B.J. Kagle (Dover, New York, 1963).

[9] G. Treglia, F. Ducastelle, and D. Spanjaard, J. Phys. (Paris) **41**, 281 (1980).
[10] S. Doniach and E. H. Sondheimer, *Green's Functions for Solid-State Physicists* (Benjamin, Reading, MA 1974).
[11] K.C. Kang, Y.-R. Jang, and B.I. Min, J. Korean Phys. Soc. **25**, 254 (1992).
[12] J.J. Yeh and I. Lindau, At. Data Nucl. Data Tables **32**, 1 (1985).
[13] S. Hüfner and G.K. Wertheim, Phys. Lett. **51A**, 299 (1975).
[14] S.-J. Oh, J.W. Allen, I. Lindau, and J.C. Mikelsen, Phys. Rev. B **26**, 4845 (1982).
[15] Y. Sakisata, T. Komeda, M. Onchi, H. Kato, S. Masuda, and K. Yagi, Phys. Rev. B **36**, 6383 (1987), and references therein.
[16] G. Treglia, M.C. Desjonqueres, F. Ducastelle, and D. Spanjaard, J. Phys. C **14**, 4347 (1981); G. Treglia, F. Ducastelle, and D. Spanjaard, J. Phys. (Paris) **43**, 341 (1982).
[17] J.K. Lang, Y. Baer, and P.A. Cox, J. Phys. F **11**, 121 (1981).
[18] D.M. Wieliczka, C.G. Olson, and D.W. Lynch, Phys. Rev. Lett **52**, 2180 (1984).
[19] O. Gunnarsson and K. Schönhammer, Phys. Rev. B **28**, 4315 (1983); **32**, 4815 (1985); in *Handbook on the Physics and Chemistry of Rare Earths*, edited by K.A. Gschneidner, L. Eyring, and S. Hüfner (North-Holland, Amsterdam, 1987), Vol. 10, p. 103.
[20] J.W. Allen, S.-J. Oh, O. Gunnarsson, K. Schönhammer, M.B. Maple, M.S. Torikachvili, and I. Lindau, Adv. Phys. **35**, 275 (1987).
[21] M.R. Norman, D.D. Koelling, A.J. Freeman, H.J.F. Jansen, B.I. Min, T. Oguchi, and L. Ye, Phys. Rev. Lett **53**, 1673 (1984); A.J. Freeman, B.I. Min, and M.R. Norman, in *Handbook on the Physics and Chemistry of Rare Earths* (Ref. 19), Vol. 10, p. 165.
[22] D.W. Lynch and R.D. Cowan, Phys. Rev. B **36**, 9228 (1987).
[23] F. Gerken, A.S. Flodstrom, J. Barth, L.I. Johansson, and C. Kunz, Phys. Scr. **32**, 43 (1985).
[24] G.D. Mahan, *Many-Particle Physics* (Plenum, New York, 1986), p. 746.
[25] C. Laubschat, E. Weschke, C. Holtz, M. Domke, O. Strebel, and G. Kaindl, Phys. Rev. Lett. **65**, 1639 (1990).
[26] E. Weschke, C. Laubschat, R. Ecker, A. Höhr, M. Domke, and G. Kaindl, Phys. Rev. Lett. **69**, 1792 (1992).
[27] S. Tanuma, C.J. Powell, and D.R. Penn, Surf. Sci. **192**, L849 (1987); D.R. Penn, Phys. Rev. B **35**, 482 (1987).
[28] L.Z. Liu, J.W. Allen, O. Gunnarsson, N.E. Christensen, and O.K. Andersen, Phys. Rev. B **45**, 8934 (1992).
[29] B.I. Min, J.-S. Kang, J.H. Hong, S.W. Jung, J.I. Jeong, Y.P. Lee, S.D. Choi, W.Y. Lee, C.J. Yang, and C.G. Olson, J. Phys. Condens. Matter **5**, 6911 (1993).
[30] F. Patthey, J.-M. Imer, W.-D. Schneider, Y. Baer, B. Delley, and F. Hullinger, Phys. Rev. B **36**, 7697 (1987).
[31] S.-J. Oh, S. Suga, A. Kakizaki, M. Taniguchi, T. Ishii, J.-S. Kang, J.W. Allen, O. Gunnarsson, N.E. Christensen, A. Fujimori, T. Suzuki, T. Kasuya, T. Miyahara, H. Kato, K. Schönhammer, M.S. Torikachvili, and M.B. Maple, Phys. Rev. B **37**, 2861 (1988).
[32] For $CeNi_2$, Refs. 19 and 20 have shown that, by using essentially the same sets of parameters, the relative weights of the peaks in the experimental spectra, obtained by $3d \rightarrow 4f$ x-ray absorption spectroscopy, $3d$ x-ray photoelectron spectroscopy, $4f$ PES, and BIS (bremsstrahlung isochromat spectroscopy), are rather well described with the calculated Kondo temperature T_K of ~ 1000 K, which is of the same order of magnitude as the experimental value of T_K.
[33] Because the fraction of the *surface* to *bulk* emission in the R $4f$ spectra is not examined for our data, care must be taken in drawing such an argument. Besides, we have not measured spectra for pure R metals with instrumental conditions the same as those for RM_2, and so there might be uncertainties in the Fermi level calibrations between Ref. 23 and our results.
[34] W.A. Harrison, Phys. Rev. B **28**, 550 (1983).
[35] W.A. Harrison and G.K. Straub, Phys. Rev. B **36**, 2695 (1987).
[36] O.K. Andersen and O. Jepsen, Physica B **91**, 317 (1977).
[37] W.A. Harrison, Phys. Rev. **181**, 1036 (1969).
[38] U. Fano, Phys. Rev. **124**, 1866 (1961).
[39] W. Speier, J.C. Fuggle, P. Durham, R. Zeller, R.J. Blake, and P. Sterene, J. Phys. C **21**, 2621 (1988), and references therein.
[40] T.-U. Nahm, M.-S. Han, S.-J. Oh, J.-H. Park, J.W. Allen, and S.-M. Chung, Phys. Rev. Lett. **70**, 3663 (1993).
[41] D.E. Eastman, F.J. Himpsel, and J.A. Knapp, Phys. Rev. Lett. **44**, 95 (1980).
[42] D. Chandesris, J. Lecante, and Y. Petroff, Phys. Rev. B **27**, 2630 (1983).
[43] E. Antonides, E.C. Janes, and G.A. Sawatzky, Phys. Rev. B **15**, 1669 (1977).